UNIVERSITY OF HELSINKI REPORT SERIES IN PHYSICS

HU-P-D115

EXPERIMENTAL STUDIES ON DIAMOND-LIKE CARBON AND NOVEL DIAMOND-LIKE CARBON - POLYMER - HYBRID COATINGS

Mirjami Kiuru

Accelerator Laboratory
Department of Physical Sciences
Faculty of Science
University of Helsinki
Helsinki, Finland

ACADEMIC DISSERTATION

To be presented, with the permission of the Faculty of Science of the University of Helsinki, for public criticism in the auditorium E204 of Physicum, on August 20th, 2004, at 12 o'clock.

HELSINKI 2004

Cover photo: Oil droplet sliding on the surface of
diamond-like carbon - polydimethylsiloxane
-hybrid coating and leaving no trace.

ISBN 952-10-1659-0 (printed version)
ISSN 0356-0961
Helsinki 2004
Yliopistopaino

ISBN 952-10-1660-4 (PDF version)
http://ethesis.helsinki.fi/
Helsinki 2004
Helsingin yliopiston verkkojulkaisut

M. Kiuru: **Experimental studies on diamond-like carbon and novel diamond-like carbon - polymer - hybrid coatings**, University of Helsinki, 2004, 36 p.+appendices, University of Helsinki Report Series in Physics, HU-P-D115, ISSN 0356-0961, ISBN 952-10-1659-0 (printed version), ISBN 952-10-1660-4 (PDF version)

Classification (INSPEC): A8100
Keywords (INSPEC): diamond-like carbon, tetrahedral amorphous carbon, filtered pulsed arc discharge (FPAD) method, adhesion, quality, plasma energy, novel coatings, hydrophobic phenomena, contact angle, sliding angle

ABSTRACT

The properties of the diamond-like carbon (DLC) coatings prepared with the filtered pulsed arc discharge (FPAD) method developed in our laboratory are exceptional; they are high-quality (>80% sp^3 diamond bonds), ultra-thick (up to 200 μm) and have excellent adhesion. These features, especially the thickness of the coating, are essential in applications. Typically the thickness and the quality of the DLC coating or thin film are compromised to avoid poor adhesion due to the internal stress in the coating. Superior adhesion is achieved with the FPAD method, where carbon ions have high energies and they form a mixing layer between the substrate and the coating. The deposition process was studied in detail and a simple and fast new method to simultaneously test the adhesion and quality of the DLC coating was developed and is reported in this thesis. Another indication of the exceptionality of the deposition system was obtained when the light emitted by the plasma in the FPAD system was studied with a spectrograph. This revealed that the energies (from Doppler shifts) and charge-states (line spectra of carbon) of the carbon ions differ significantly from those of reported in the literature. The carbon ions in the FPAD plasma have higher energies and higher charge-states than those typically reported for carbon ions.

The benefits of using tantalum as an intermediate layer between the substrate material and the DLC coating are discussed in this thesis. The tantalum layer was first introduced as it improved the adhesion and allowed a wider variety of substrate materials to be used. At present, the use of tantalum is recommended to prevent pinhole failure. In a corrosion experiment with tantalum coated and uncoated human hip joint prostheses it was found that when exposed to 10% HCl solution tantalum coating decreased the corrosion rate of CrCoMo acetabular cups by a factor of 10^6.

The modification of the FPAD method to prepare novel DLC-polymer-hybrid coatings is also covered in this thesis. Both the coatings and their deposition method are recent innovations of our research group. In the novel coatings the properties of the polymer and the hard DLC can be combined. Common non-stick polymers, polydimethylsiloxane (PDMS) and polytetrafluoroethylene (PTFE), have been used as the polymer component in the hybrid coatings and as a result coatings that are considerably hard and water and oil repellent have been prepared. The water and oil repellency is observed in the high contact angles of water and oil on the surface of the coating and also in the sliding angle measurements: water and oil droplets leave no visible trace on the surface of the hybrid coatings and with DLC-PDMS-hybrid coating an extremely low sliding angle of only 0.15°±0.03° was measured with a 20 μl distilled water droplet (the lowest sliding angle value given in the literature is 1°).

CONTENTS

LIST OF PUBLICATIONS

This study consists of a summary and the following papers published in international scientific journals with a referee system. The references to these papers will be denoted by Roman numerals.

I **Adhesion and quality test for tetrahedral amorphous carbon coating process,** E. Alakoski, M. Kiuru, V-M. Tiainen, A. Anttila, Diamond Relat. Mater. **12**, 2115 (2003).

II **Tantalum as a buffer layer in the diamond like carbon coated artificial hip joints,** M. Kiuru, E. Alakoski, V-M. Tiainen, R. Lappalainen, A. Anttila, J. Biomed. Mater. Res. Part B: Appl. Biomater. **66**B, 425 (2003).

III **Energies and charge-state fractions of carbon plasma ions measured with Doppler-shifts in the pulsed arc-discharge system**, V-M. Tiainen, E. Alakoski, M. Kiuru, A. Soininen, A. Anttila, Eur. Phys. J. Appl. Phys. **22**, 111 (2003).

IV **Preparation of diamond-like carbon - polymer hybrid films with filtered pulsed arc discharge method**, A. Anttila, V-M. Tiainen, M. Kiuru, E. Alakoski, K. Arstila, Surf. Eng. **19**, 425 (2003).

V **Low sliding angles in hydrophobic and oleophobic coatings prepared with plasma discharge method**, M. Kiuru and E. Alakoski, Mater. Lett. **58**, 2213 (2004).

The research presented in this thesis is a result of group work. The author's main contribution has been participating in the development and operation of the deposition system as well as in the sample preparation and analysis (I-V). The author conducted the surface topography measurements in Papers I, IV and V. In Paper II, the author was responsible for the sample preparation for the PIXE measurements and the analysis. In Paper III, the author participated in the construction of the optical measurement apparatus and its calibration and during the measurements the author participated in the film developing and analysis. In Papers IV and V, the author conducted the contact and sliding angle measurements. The author of this thesis was engaged in writing of all of these papers, and she was the corresponding author in Papers II and V. The work was carried out by the Helsinki University Diamond Group using the facilities of the Accelerator Laboratory at University of Helsinki. The Helsinki University Diamond Group is part of a Center of Excellence appointed by the Academy of Finland (Medical, Dental and Veterinary Biomaterials Research Group).

1 INTRODUCTION

The first diamond-like carbons (DLC's) were prepared in the beginning of the 1970s when Chabot and Aisenberg used the direct ion beam deposition to prepare DLC thin films [1]. Since then the pursuit to harness the exceptional properties of natural diamond, such as high mechanical hardness and chemical inertness, in coatings has been ongoing (see Table 1). DLC is a viable material for wear-resistant applications such as the protective coatings on magnetic hard disks and their reading heads, cutting tools, automotive components and orthopaedic prostheses [2-11,II].

In wider industrial use the price of the coating plays an important role. The price of the resulting coating depends on the deposition method and its efficiency. Thus, for practical applications a deposition method with a high deposition rate is needed. For example, the method applied to prepare the first DLC's had a low deposition rate and is therefore only suitable for laboratory use.

It has been found that DLC's properties similar to those of diamond are achieved in an isotropic disordered thin film with no grain boundaries [12]. This excludes the chemical vapor deposition (CVD) methods where thin films consisting of small crystallite diamonds are formed via a chemical process from various gaseous hydrocarbons. These films have a high hydrogen content (20-50%), their surface is quite rough because of the crystallites and consequently they have weaknesses due to the grain boundaries.

Table 1. Some properties of diamond [13] vs. high-quality DLC [12,14-17].

	Amount of sp^3 diamond bonds	Hardness (GPa)	Density (g/cm^3)	Resistivity (Ωcm)
Diamond	100%	100	3.515	10^{20}
High-quality DLC	>80%(*)	70-80	3.1-3.5	10^{9}-10^{11}

(*) Determined with electron energy loss spectroscopy (EELS).

The Helsinki University Diamond Group, led by Prof. Asko Anttila, has been studying DLC coatings since the 1980s [5-9,18-27]. With the filtered pulsed arc discharge (FPAD) deposition method developed in the laboratory superior DLC coatings can be prepared. FPAD is a physical vapor deposition (PVD) method, which utilizes high-energy carbon plasma beams yielding high deposition rates, thus making it also suitable for industrial use. The coatings prepared with FPAD are amorphous (the carbon atoms that form these coatings are isotropically disordered and no grain boundaries exist), ultra-thick (up to 200 μm), high-quality (amount of sp^3 diamond bonds >80%) and well-adherent. It should be clarified here, that the term 'high-quality' in context with the DLC coatings refers to the high amount of sp^3 diamond bonds in the coating.

To reach a thickness of 200 μm for a high-quality DLC film is exceptional and as far as we know coatings with these properties have not been prepared elsewhere in the world. Typically the thicknesses of the coatings (or thin films when thicknesses are less than a micron) are orders of magnitudes thinner. For instance, Chhowalla [4] reported that the internal compressive stress in the high-quality DLC film rose rapidly to ~10 GPa as the film thickness exceeded 10 nm. The stress saturated at that maximum value in films with thicknesses of 20-100 nm and after this the stress dramatically decreased as delamination occurred. The same kind of stress behavior of DLC film from 0 to 10 nm was also reported in Ref. [28].

Carbon is a very versatile element as it can form bonds in several different ways and thus it is found in many different materials. Carbon forms a variety of crystalline and disordered structures, because it has three different bonding configurations (Figure 1) [29]. In the nature elemental carbon is usually found in one of its two allotropic forms, viz. graphite and diamond. In diamond, the carbon atom's four valence electrons are each assigned to a tetrahedrally directed sp^3 orbital, which makes a strong covalent bond with an adjacent atom. In graphite, three valence electrons enter trigonally directed sp^2 orbitals and form covalent bonds. The fourth valence electrons form a 2D electron gas and the sp^2 bonded planes interact via weak Van der Waals forces. The strong and equivalent covalent sp^3 bonds in diamond explain its extreme physical properties. In graphite the weaker bonds between the covalently bonded planes explain its brittleness and also its use as a solid lubricant because its covalently bonded planes are able to move with respect to each other.

In the sp^1 configuration the covalently bonding electrons are in orbitals directed along the x-axis while the other two electrons are along y and z directions and forming weaker bonds.

In the diamond crystal structure carbon atoms are densely packed: the lattice is fcc (face-centered cubic) Bravais lattice with a basis of two [13]. In amorphous DLC coating, the carbon atoms are arranged so that no long range order is present. To give an idea of this kind of structure (a carbon system with 80% sp^3 bonds), a computer simulation to model the structure is presented in Figure 2 [30]. The figure shows that the structure consists of a net of carbon atoms bonded in various directions with no long range order.

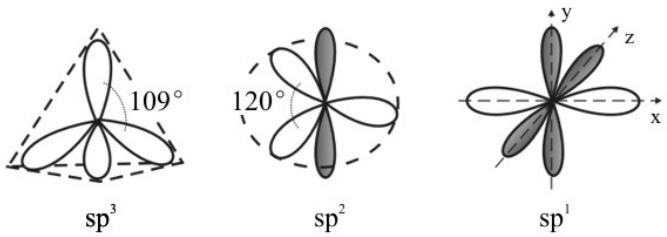

Figure 1. The three different bonding configurations of carbon.

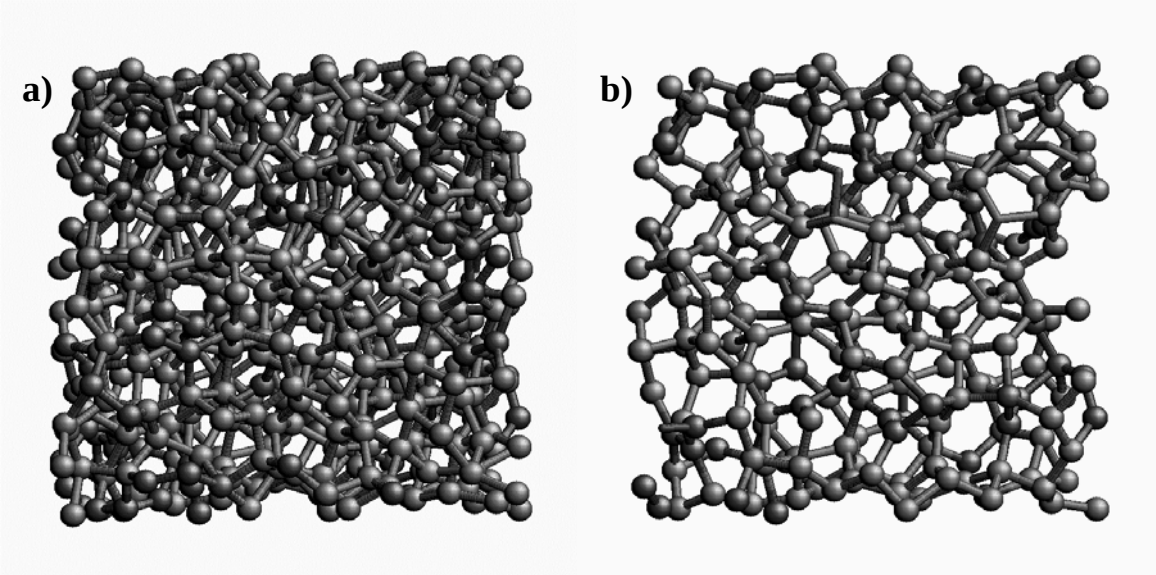

Figure 2. a) Computer simulation of the structure of DLC (512 carbon atoms in a system with about 80% sp^3 bonds) [30]. **b)** For clarity only half of the structure presented in a) is shown. In the simulation the cells were made with the Brenner II hydrocarbon potential [31], starting from random atom coordinates at high pressures and temperatures that were then slowly cooled down to 300 K and ambient pressure in several stages.

The ambiguity of the nomenclature concerning DLC is worth mentioning here. In a recent review J. Robertson defined: “Diamond-like carbon is a metastable form of amorphous carbon (a-C) containing a significant fraction of sp^3 bonds”[12]. However, the term DLC has been used as a general term for carbon coatings with some diamond-like bonding. It does not guarantee high or even a significant sp^3 fraction and thus the term tetrahedral amorphous carbon (ta-C) has been suggested [16,32] for DLC with high sp^3 fraction to distinguish it from the sp^2 bonded a-C. A contradictory term, amorphous diamond (AD), has also sometimes been used. The term draws attention to itself, because it points out the exceptionality of the material, but it has been disputed since diamond is the term for a distinct crystal structure far from amorphous [17].

In Papers I-III, the terms tetrahedral amorphous carbon (ta-C) and diamond-like carbon (DLC) are both used, but in papers published in physical journals ta-C is preferred. In Papers IV and V, DLC was chosen for the new term to describe the novel hybrid coatings, because the DLC-polymer-hybrid (DLC-p-h) coatings can have quite a low amount of ‘diamond component’ in them if the amount of polymer component is raised. In this summary, the term diamond-like carbon (DLC) is used instead of tetrahedral amorphous carbon (ta-C) for simplicity.

Overall, the exceptional properties of the DLC and DLC-polymer-hybrid (DLC-p-h) coatings and their preparation methods are discussed in this thesis. The motivation for this study was to develop the deposition system and to understand the processes that take place during the deposition. In Paper I, the superior adhesion and high-quality of the DLC coating prepared in our laboratory is demonstrated and a simple and fast method to test these properties is presented. Paper II focuses on one of the applications of DLC coatings, viz. artificial hip implants, and proves that the use of tantalum as an intermediate layer between the substrate and the coating is highly beneficial. In Paper III, the energies and charge-states of the carbon plasma generated in our deposition system are examined and the results are found to differ significantly from the results obtained with other arc discharge plasmas. Papers IV and V present the results of pioneering research work aiming at novel diamond-like carbon - polymer -hybrid coatings.

2 THE DEPOSITION PROCESS OF DIAMOND-LIKE CARBON

2.1 The filtered pulsed arc discharge (FPAD) method

The deposition method used in our laboratory for preparing DLC coatings is the filtered pulsed arc discharge (FPAD) method [20]. With slight modifications the FPAD unit is also suitable for the deposition of DLC-p-h. A schematic representation of the FPAD unit is shown in Figure 3.

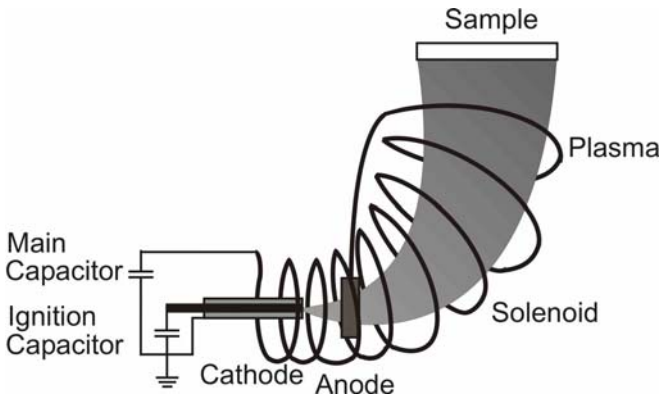

Figure 3. A schematic representation of the FPAD unit.

When preparing DLC with FPAD a graphite cathode is used. The FPAD unit is in a vacuum at a pressure of about 100 μPa and in order to create carbon plasma an arc similar to lightning is generated from the surface of the graphite cathode by discharging the ignition capacitor bank (C=10-20 pF). This causes electrons and carbon ions (plus unwanted neutral carbon atoms and larger particles) to ‘explode’ out of the cathode [21]. The cathode is worn in this violent process and its wearing effects the generation of plasma in the following pulses and therefore the cathode is usually rotated and the surface is cleaned continuously by abrading it against an alumina sheet [22]. The plasma generated in the arc discharge then encounters a ring shaped graphite anode, which is at a higher potential (U=500-6000 V). As the plasma (lighter electrons first and the heavier carbon ions after) reaches the anode, the main capacitors are discharged. The main RCL-circuits

parameters are typically the following: the tuning resistor R≈0.1 Ω, main capacitor capacitance C≈10-30 μF, filtering solenoid inductance L ≈ 3 μH. The current (in the order of several kA) from the main capacitors is led through a curved solenoid and a synchronized magnetic field (~1 T) is created to steer the plasma towards the sample and to filter out the unwanted neutrals and larger particles. The pulse frequency can be tuned from f=0-10 Hz. The ignition capacitor bank is discharged when the voltage is high enough (~2 kV) and striking occurs in the breaker gap, short-circuiting the ignition circuit. The breaker gap can be adjusted and thus controls short-circuiting and the pulse frequency.

With the FPAD method, energetic plasma pulses with a high ion density can be generated. From the volume and density of the deposited DLC coating and the deposition time, one can estimate the average current the plasma carries in the FPAD to be in the order of amperes. The FPAD method is a fast method to produce DLC; the maximum deposition rate is 6 μm/h for an area of 25 cm^2 and coatings as thick as 200 μm have been deposited. The high deposition rate facilitates the industrial use of the method. The 200 μm DLC coating was deposited in our laboratory for pure scientific interest only, but nevertheless to our knowledge it is the world record for thickness of DLC coating. However, for practical applications a thickness of a couple of tens of microns is sufficient.

2.2 Substrate properties

Several factors need to be taken into account when starting a FPAD deposition. The key factor limiting the use of DLC coatings is the lack of adhesion between the substrate and the coating. Therefore, the sample material has to be carefully considered: the substrate has to be ”soft” enough (Vickers hardness, H_V<3 GPa) [23]. If the substrate material is hard (H_V>3 GPa) the deposited DLC coating easily peels off the substrate because of the high internal stress of the coating (compressive internal stress can be up to 10 GPa [4,24,28]). In addition to proper hardness, the substrate material should be a carbide forming material. For example, copper is soft enough, but it does not form carbides and therefore direct deposition of DLC on it fails. Using carbide forming materials, such as tantalum, as intermediate layers thick (≥100 μm) DLC coatings can be prepared [23]. Furthermore, if the substrate material is soft the possibility that the substrate material will be deformed

under the highly stressed DLC coating has to be taken into account. This is the case with e.g. a copper substrate when a several millimeter thick copper plate is bent under a thick (several tens of microns) DLC coating. A typical well-behaving and commonly used substrate material is stainless steel AISI316L.

Before depositing the coating, the geometry of the sample has to be considered and a proper sample holder has to be designed (samples can be rotated during deposition to reach all sides on the sample). If the sample has sharp edges there is a risk that the coating will not properly adhere onto these areas because the internal stress in the coating accumulates on these areas.

In Paper I, a simple method to test the adhesion and quality of DLC coating is presented. The test is largely based on facts explained in the previous paragraph and the observation that the compressive internal stress of DLC coating can break and peel off the surface of the silicon wafers [24]. Hard, but carbide forming silicon is used for the deposition of DLC. Because silicon is a hard and brittle ceramic material, the DLC coating will eventually peel off the surface and, if the adhesion is good, the deposited coating will peel off and break the substrate. The peeling off effect is typically measured with a profiler (Figures 4 and 5, see also Figures 2 and 3 of Paper I). The interpretation of these events is consistent: first, if the coating peels off without breaking the substrate, the adhesion is insufficient. Secondly, if the coating peels off and breaks the substrate, the adhesion is good and the peeling thickness indicates the quality of the DLC: the thicker the coating was before the break down occurred, the poorer the quality (lower internal stress) of DLC. For instance, the amount of sp^3 bonds in a sample with peeling thickness of 0.5 μm was 85% and with 1.5 μm it was 80% [I].

The calibration samples of this method were measured with X-ray photoelectron spectroscopy (XPS) in order to establish the amount of sp^3 bonds in them. XPS measurements are rather expensive and time-consuming and thus can be performed only on special occasions. Another method often applied in our laboratory to measure the quality of the coating is electronic resistivity measurement, based on the fact that the resistance of the coating increases as a function of the quality. This method is simple and fast for quality determinations but of course useless for adhesion determinations.

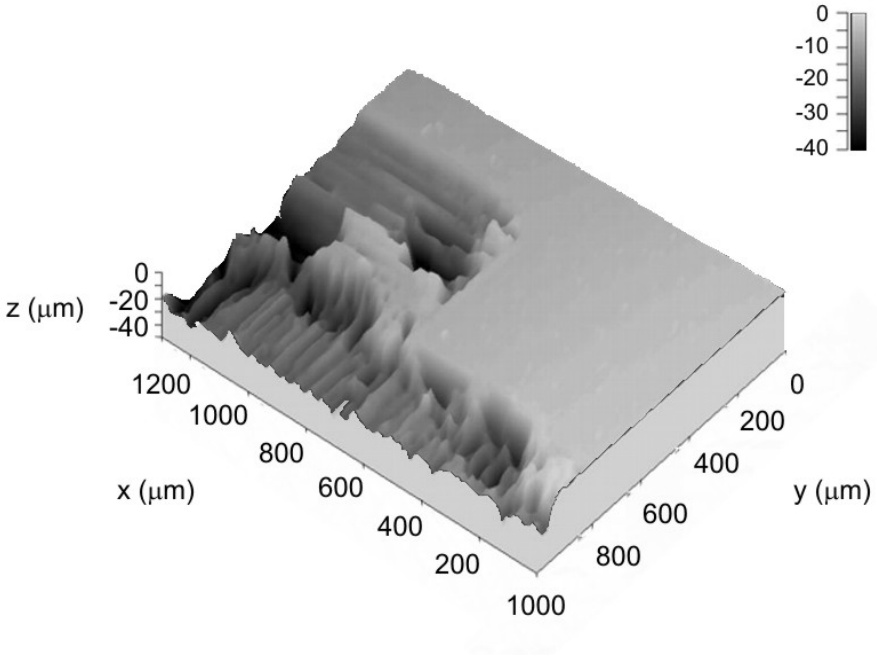

Figure 4. 3D scan of a sample with about 1 μm thick DLC coating on Si substrate. The DLC has been peeled off and the silicon substrate has thereby been damaged.

Figure 5. The scan in Figure 4 was performed with a 3D stylus profiler (KLA Tencor P-15) in a clean room environment at the University of Helsinki Department of Physical Sciences.

2.3 Sample cleaning

Before deposition the sample is, when necessary, polished (a substrate roughness of about 50 nm is sufficient). This is followed by chemical cleaning with acetone and ethyl alcohol in an ultrasonic washer. Next, pressurized nitrogen is used to remove particles from the sample surface. The sample is then placed in the vacuum chamber and it is sputtered with high purity (99.999%) argon. In sputtering, atoms from target are ejected because of collision events caused by ion impacts on the target. The sputtering yield naturally depends on the sample material and the energy and mass of the sputtering ion. For instance, for argon with an energy of 0.5 keV the sputtering yield is 1.05, 1.10, 1.22 and 0.50 atoms/ion for Al, Fe, Co and Si, respectively [33]. For cleaning purposes a couple of atomic layers to several hundreds of nanometers can be removed with sputtering. The sputtering cleaning process is usually about a ten minutes task with our DC sputtering apparatus (4 kV, 20 mA). Argon sputtering removes e.g. an undesired layer of adsorbed water (instantly formed from ambient air before the sample is placed into the vacuum) from the surface of sample.

2.4 Tantalum intermediate layer

The intermediate tantalum layer was originally introduced since it enhanced the adhesion between the substrate and the DLC coating. Using a tantalum layer, a wider variety of substrate materials can be coated. The intermediate tantalum layer is deposited with a magnetron sputtering apparatus. In the magnetron sputtering apparatus the electrons emitted from the cathode are accelerated towards the anode but are then trapped in a magnetic field parallel to the target surface and left spinning there, enhancing the ionization of the working gas. The ionized working gas, in our case argon with purity of 99.999% at a pressure of 2 Pa, sputters the tantalum target and as a result a tantalum coating is formed on a substrate. With this method high deposition rates are achieved. The plasma power is about 700 W (U≈400-600 V and I≈1-2 A) and the base pressure in the vacuum chamber is ~10^{-4} Pa. The purity of the tantalum target used in our system is 99.99%; the main impurity being niobium and the deposition rate achieved is 0.4 μm/min.

It is known that bulk tantalum is “soft” (H_V=1.1 GPa) and chemically very corrosion resistant [34] but it has been reported that tantalum is somewhat difficult to deposit and that it has a tendency to form hard and brittle phases [35,36]. Despite this, the deposition of tantalum with magnetron sputtering was successfully carried out in our laboratory. In Paper II it was demonstrated that in addition to improved adhesion a tantalum layer is useful as it increases the corrosion resistance of the coating (patent pending, [37]).

The use of a 4-6 μm thick tantalum coating on CrCoMo acetabular cups (cup part of the human hip joint prostheses) decreased the corrosion rate by a factor of 10^6 when tantalum coated and uncoated cups were exposed to a 10% hydrochloride acid (HCl) solution at room temperature. Drops of the HCl solution from the cups were taken after different periods of exposure and they were allowed to dry on a 2 μm Kapton® foil. The amount of dissolved chromium, cobalt and molybdenum were measured from these samples with proton induced X-ray emission (PIXE) [38-40]. PIXE is a very sensitive method (accuracy of ppm is easily achieved) for elemental analysis. In PIXE, a proton beam targeted on the sample excites the electrons on the inner *K* and *L* shells of the atom and when deexcitation occurs X-ray radiation is emitted. Thus, X-rays with characteristic energies corresponding to the atom that emitted it can be detected. The probabilities for a fluorescence photon to be emitted are known (the intensities of characteristic X-ray emission lines) and the amounts of different elements can be determined using standard specimens. In Paper II, an inner standard element (Se) was added to the samples before PIXE measurements.

The increase in the corrosion resistance of the coating with tantalum intermediate layer can be explained by understanding the failure mechanism caused by a pinhole in the coating. A microscopic hole in the coating, i.e. pinhole, can be formed in the coating, e.g. if a dust particle is left on the surface of a sample after cleaning. In a hostile environment the substrate material can be dissolved through a pinhole, which can cause crack formation. In the case of a coating with high internal stress, interface cracks can lead to the complete delamination of the coating. The pinhole effects can be avoided by preparing thicker (tens of microns) DLC coatings and by using an intermediate layer that is corrosion resistant to protect the substrate material.

Of course, in addition to corrosion resistance, other properties of the material in the intermediate layer have to be compatible. In Paper II, the intermediate layer is used in the diamond-like carbon coated artificial hip joints, which sets even more demands on the material. Tantalum was chosen for this task since it fulfills all the requirements, e.g. good adhesion to both the substrate and the DLC coating, suitable hardness, good fatigue properties under long lasting mechanical cyclic stress and insolubility in body fluids and biocompatibility [34,41].

2.5 High-energy deposition

The deposition system (Figure 6) consists of two FPAD units, one for the purpose of producing high-energy plasma and the other for carbon plasma with a lower energy. The deposition of the actual DLC coating begins with the high-energy carbon plasma in order to create an intermediate adhesion layer (10-50 nm) where carbon atoms are mixed into to substrate and if possible, carbide is formed. The high-energy FPAD unit has high anode-cathode voltage (6 kV) and high peak current (13 kA). The pulse duration is short (15 μs). In the high-energy deposition the plasma ion energy is significantly higher (200-600eV) than the ion energy required to achieve the maximum fraction of sp^3 bonds [25-27,III] and this unit produces low-quality coatings (sp^3 fraction about 40%). Thick well-adherent DLC coatings can be easily prepared onto some soft carbide forming materials such as bulk aluminum and bulk titanium without any intermediate layers (tantalum or carbon deposited with high-energy), but for example on stainless steel (AISI 316L) thick coatings fail without high-energy adhesion layer.

2.6 Low-energy deposition

The low-energy FPAD unit is used for preparing the actual high-quality (>80% sp^3 bonds) DLC coating. The ion energy is a crucial parameter for obtaining sp^3 bonds and therefore, the energy of the carbon ions in the low-energy FPAD unit is optimal for this $E \approx 100$ eV [16,17,27,42,43]. The low-energy unit is similar to the high-energy unit, except that the arc discharge voltage is lower (500 V) and the pulse duration is longer (60 μs).

Figure 6. Plasma deposition system at the University of Helsinki Accelerator Laboratory. Attached to the vacuum chamber are: on the left is the argon sputtering unit; straight ahead the high-energy deposition unit; on the right are the turbo and oil diffusion vacuum pumps.

2.7 The energies and charge-states of carbon ions in the plasma

The energies of the carbon ions in the arc discharge plasma have been measured in our laboratory with the time-of-flight (TOF) method [25,26]. The principle of this method is to measure the flight time of the ions between two observation points of known distance. In our measurement system this is accomplished by observing the light the plasma emits: optical fibers are placed into the vacuum chamber to look over two points inside the solenoid, the fibers lead the light to pin-diodes and the signal from them is amplified and read from the oscilloscope.

The TOF apparatus is simple and quick to build and use, but its disadvantage is that its accuracy decreases as the ion energies increase. Thus, another method for energy determination was needed. Measuring the speed of a plasma pulse (pulse duration 10-60 μs) in vacuum is a complicated task and even the measuring apparatus easily disturbs the plasma. Also, any electronic measuring apparatus can get damaged because of the electromagnetic pulses (EMP) generated by the arc discharge unit. The disturbance is

negligible when only the light the plasma emits is observed. The energy of the carbon ions was measured by studying the Doppler shifts in the line spectra emitted by carbon plasma. In Paper III, the energies and the charge-states of carbon ions in the plasma discovered from the line spectra data are reported. The results were exceptional, especially in the case of the charge-states, because multiply charged carbon ions were detected.

The Doppler shift method is based on the Doppler effect: the frequency (and wavelength, $\lambda=c/f$) of light is altered if the sender of the light is in motion. If the sender of the light moves with velocity of v ($v<<c$, velocity is much smaller than the speed of light) the wavelength λ of the light it emits is altered to λ' [44]:

$$\lambda' = \lambda\left(1 \pm \frac{v}{c}\cos\theta\right). \quad (1)$$

When the sender is approaching the observer with velocity v, the light is blue shifted to smaller wavelengths and '-' sign is applied in the equation. When the sender is receding from the observer, the light is red shifted to larger wavelengths and '+' is applied. The angle θ has to be taken into account if the movement of the sender is not straight towards or away from the observer (θ is the deviation from this).

The carbon ions in the plasma are in motion and they emit light characteristic of the carbon atom. The characteristic wavelengths are a discrete set of spectral lines formed out of the transitions of electrons between quantized energy states (in deexcitation a photon is emitted) of corresponding atom and can be observed with the help of spectrograph. The characteristic wavelengths of carbon, including neutral atom and its different ionization states, are well known. Also, the intensities of the lines are known to some extent.

A schematic representation of the apparatus for measuring the line spectra of the carbon plasma and the Doppler shifts is presented in Figure 7. The light emitted by the carbon plasma is guided from the vacuum chamber to the spectrograph using optical fibres. The fibres can be set to different angles in respect to trajectory of the plasma, and depending on these angles the Doppler shifts are be observed. A special fibre stand was designed and built for this purpose. In the crossed dispersion spectrograph glass optics are used, including several mirrors and a grating (300 lines/mm). The spectra are recorded on a film.

The fibre stand allows the use of a reference light source, and the output of the spectrograph was first calibrated using argon and helium discharge lamps. However, this is not necessary for every measurement since the Doppler shifts can be calculated from the difference between shifts of the same line from different fibres, e.g. at +45° and -45° angle in respect to the plasma (see Paper III, Figures 2 and 3). The wavelength range that can be detected with this apparatus is limited by its components: the working range of the spectrograph is 370-550 nm and the useful detection range of the film is from 350 to 520 nm (the fibres caused no limitation in this wavelength range).

After recording the spectra on film, the photographs were studied with a CCD-videomicroscope and transferred to a computer. The images were then analyzed with an image processing tool and the centroids and the intensities were calculated from the line profiles (see III, Figures 2 and 3). For instance, energy of 100 eV corresponds to a velocity of about 40 km/s and in the measurement set-up of the fibres at ±45° this would mean a $\Delta\lambda \approx 0.88$ Å difference in the shifted wavelengths of the 4647.42 Å line and on the film this leads to an approximately 0.11 mm separation in the line positions (linear dispersion 7.6 Å/mm), which is easily measured with our system.

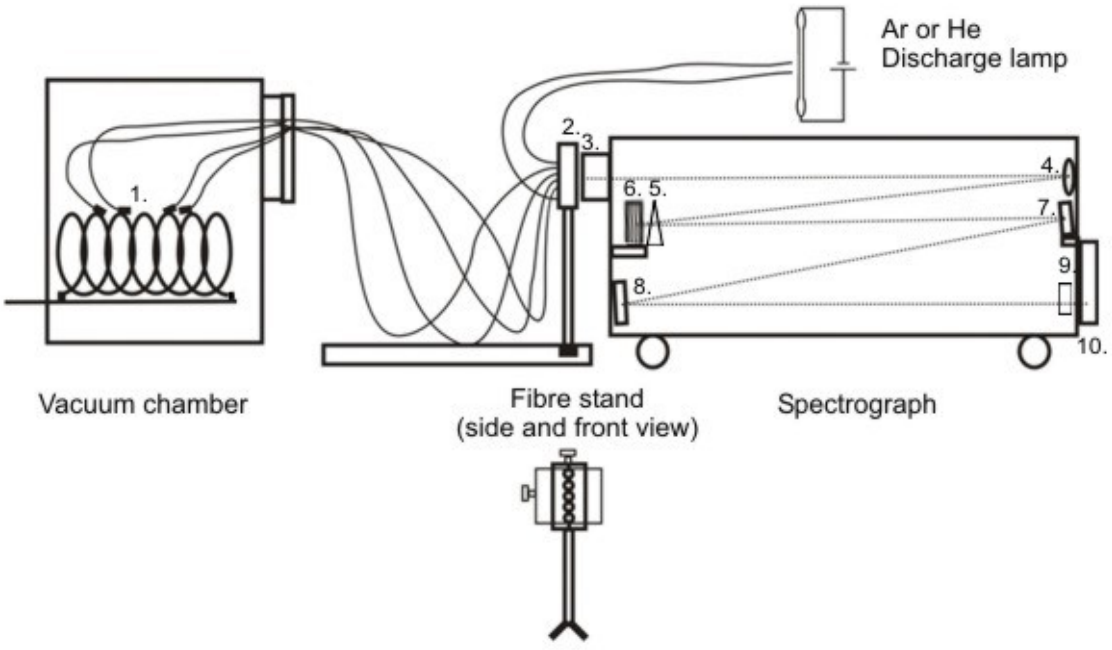

Figure 7. Measurement apparatus for the line spectra of the carbon plasma (not to scale): 1. the collimated fibres in the vacuum chamber, 2. fibre stand, 3. slit, 4. spherical mirror, 5. glass prism (separates the light into a spectrum in the vertical plane), 6. diffraction grating (separates the light into a spectrum in the horizontal plane), 7. tilting mirror, 8. spherical mirror, 9. plane-convex field lens and 10. film.

The results obtained from these measurements differ significantly from those reported in previous studies. Earlier it was thought that the single ionization state would be dominating for carbon [14,45-49], but in our measurements the ratios for carbon ions of charge-states 1+, 2+ and 3+ (or C^{+}, C^{2+} and C^{3+}) were 4, 23 and 73, respectively [III]. The abundance of different ionization states is deduced from the intensity information found in the literature [50,51], which, unfortunately, is usually rather inaccurate. The presence of C^{4+} can only be speculated, since the relative intensities of 4+ charge-state lines are very low in the working range of our spectrograph they were not observed. The ionization energy for C^{4+} is not significantly higher than that for C^{3+}[50]. The energies of the carbon ions were found to vary depending on the charge-state of the ion. The energies for carbon ions of charge-states 1+, 2+ and 3+ were 32, 110 and 250 eV, respectively. The earlier studies [14,45-49] on ionization states and their energies were obtained with arc discharge devices, but the currents used in them were significantly lower (≤200 A) than those used in our laboratory (7.5-10 kA).

3 DIAMOND-LIKE-CARBON - POLYMER -HYBRID COATINGS

In Papers IV and V the research work done concerning the discovery of novel diamond-like-carbon - polymer -hybrid (DLC-p-h, patent pending [52]) coatings are presented. The DLC-p-h coatings can be prepared with slight modifications to the FPAD deposition system. In deposition of the DLC-p-h coating a graphite-polymer cathode is used. The properties of the DLC-p-h coatings vary mainly depending on the amount of polymer component in them. It is possible to alter the amount of the polymer component in the resulting coating by changing the pulse frequency (even during deposition), which mainly controls the polymer evaporation. Using polydimethylsiloxane (PDMS) and polytetrafluoroethylene (PTFE) polymers in the deposition process, DLC-PDMS-h and DLC-PTFE-h coatings with remarkable properties are created. These polymers were chosen because they are common non-stick materials (“silicone rubber” and teflon®) and their anti-soiling properties were also desired for the novel hybrid coatings.

Non-stick and anti-soiling surfaces can be discussed using the theory of wetting and non-wetting, i.e. whether the liquid spreads on the surface or not. In this context the term hydrophobicity (water repellency) is typically used since water is such a common liquid, but other liquids such as oils (oleophobicity, oil repellency) should also be recognized. Anti-soiling properties are crucial in several applications and they have so far been pursued through extreme surface characteristics, either by creating a surface that is philic (e.g. hydrophilic, water spreads on the surface) or phobic (e.g. hydrophobic, water forms droplet on the surface) [53]. Sprays that make a surface more hydrophilic can be purchased in order to ease the cleaning of household windows or to prevent fogging in swim goggles. Hydro- and oleophobic surfaces are familiar from e.g. frying pans. In nature some plants have leaves that are highly hydrophobic. Ideas for the usage of hydrophobic surfaces include glass buildings and windows, windshields and mirrors of cars, hulls of ships, tubes or pipes and bio applications [54-61]. Also, lab-on-a-chip technology benefits from non-wetting surfaces [62]. Philic and phobic surfaces can be used in anti-soiling applications, but the benefit of a phobic surface is that it limits chemical reactions or bond formation because of the small contact area and thus it prevents various phenomena on the surface such as snow-sticking, contamination or oxidation and current conduction [54,55].

In Papers IV and V, novel hybrid coatings with exceptional properties are presented. The DLC coating is a hard (Vickers hardness 80 GPa) material with a water contact angle (see next chapter) of around 70° to 80°. When a suitable polymer is added to this during the deposition the resulting coating can have properties varying from DLC-like to polymer-like. For example, with a soft non-stick polymer, PDMS, a combination of 26 GPa Vickers hardness and 109° water contact angle in the coating was easily achieved. In fact, the DLC-PDMS-h coating was found to be an excellent non-stick coating, having high contact angles >100° and low sliding angles < 1°, and in demonstration water and oil droplets slid smoothly across the surface of the coating leaving no observable trace (see Paper V, Figure 2). The surface properties of the novel DLC-p-h coatings were analyzed with static and dynamic contact angle measurements and with sliding angle measurements as explained in the following chapters.

3.1 Static contact angle measurements

Water and oil repellency are described with the terms hydro- and oleophobicity. Whether the surface is hydro- or oleophobic, can be simply estimated by placing a small droplet (~10 µl) on the surface and measuring the contact angle θ (see Figures 8 and 9). This is called the static contact angle. If the contact angle is high, for instance over 90° in the case of water, the surface is said to be hydrophobic. With oils no strict limit exists since they tend to spread on surfaces and they have much smaller contact angles compared to water. In this situation Young's equation can be applied [63,64]:

$$\gamma_{lv} \cos\theta = \gamma_{sv} - \gamma_{sl}, \tag{2}$$

where γ_{lv}, γ_{sv} and γ_{sl} are the interfacial tensions or free energies per unit area of liquid-vapor, solid-vapor and solid-liquid interfaces, respectively, as presented in Figure 8 a).

The contact angles have been measured in our laboratory with an apparatus specially constructed for this purpose (Figure 8 b). The contact angle measurement apparatus is constructed on a stone table and it consists of an optical bench, in which the sample holder (a millimeter table that can be inclined) and a prism are attached to so that the picture of the droplet can be taken with a CCD-videomicroscope facing down. The pictures are saved to a computer where the analysis is performed with suitable software.

Common image processing software have distance and angle measuring tools which can be applied in the contact angle analysis. The static contact angles can also be examined via a geometrical approach, where the contact angle is obtained from the equation:

$$\theta = 2\arctan\left(\frac{h}{x}\right), \tag{3}$$

where h and x are height and half of the width of the droplet, respectively, as plotted in Figure 9.

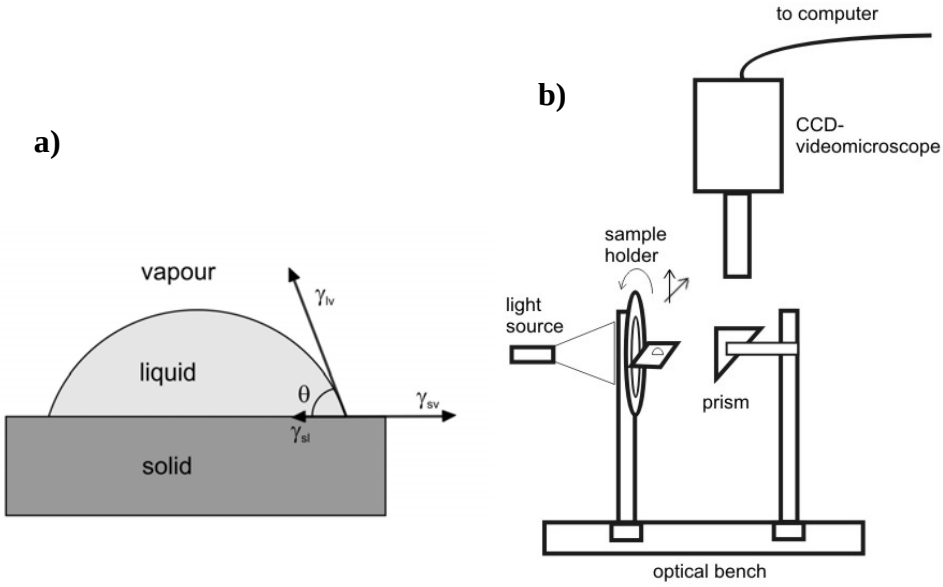

Figure 8. a) The interfacial tensions contributing to the contact angle θ of liquid droplet on solid surface. **b)** The contact angle measurement apparatus.

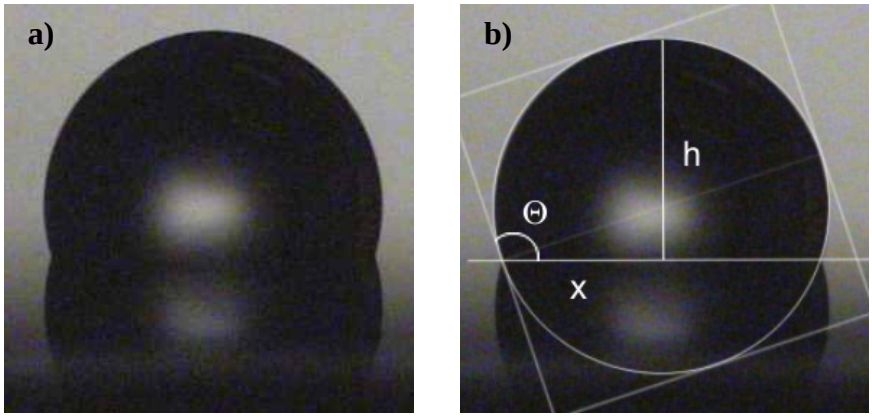

Figure 9. a) Picture of a 5 µl water droplet obtained with the CCD-videomicroscope. **b)** Contact angle analysis of the droplet.

3.2 Dynamic contact angle and sliding angle measurements

The static contact angle measurements with water and oil give the basic estimation of the hydro- and oleophobicity of the surface, but for a more detailed analysis dynamic contact angle and sliding angle measurements should be performed. In dynamic contact angle measurement the surface is inclined to a position in which the droplet moves very slowly down on the surface. In this position the maximum value for the contact angle is gained on the side of the advancing contact angle θ_A and on the other side the receding contact angle θ_R is measured (Figure 10).

The sliding angle is the critical angle at which a droplet begins to slide down an inclined plane. Our measurement apparatus is suitable for the dynamic contact angle and sliding angle measurements since the sample holder can be inclined. However, for the samples with the lowest sliding angles another apparatus with higher precision for the inclination angle was constructed.

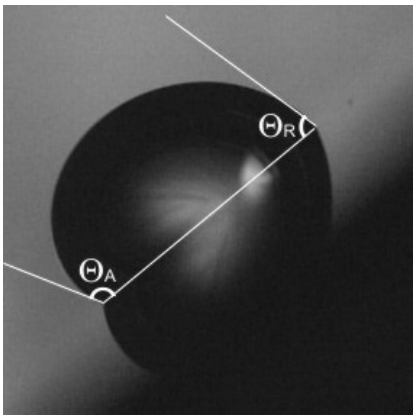

Figure 10. Dynamic contact angle measurement and the advancing and receding contact angles, θ_A and θ_R.

3.3 Effect of surface topography

Theories and studies from several decades concerning how liquids spread and move on surfaces exist and even the founding Young's law dates back to 19th century [63]. It is worth mentioning the huge impact of the surface geometry and chemical heterogeneity on

the contact angles [65-72]. In fact, a water contact angle of only around 120° is achieved with material of lowest surface energy (surface with regularly aligned closest hexagonal packed -CF_3 groups) [73], after this the increase in the contact angle is due to the surface topography. On hydrophobic surfaces roughness decreases wetting as the drop is pinned on the surface. On hydrophilic surfaces roughness increases wetting as the drops appear to sink into the surface. In the case of hydrophobic material it is also possible that air pockets are left in the roughest regions. The contact line of the drop can have complex shape because of surface geometry or chemical heterogeneity and this has its effect on contact angle.

The leaf of a lotus flower has such a surface structure combined with hydrophobic surface material that water droplets have high contact angles and they drip off the surface of leaves taking powder-like contaminants along [74]. Attempts to copy nature have been made, but problems exist, e.g. aging and decay, which do not occur in nature where leaves repair themselves. Also, if the textures of a rough surface are filled with water the material loses it water repellency [75]. The invasion can occur e.g. through an external pressure.

3.3 Anti-soiling, high contact angles and low sliding angles

Sliding angles are rarely reported in the literature. From the earlier publications only qualitative information on this subject can be found. In the preparation of anti-soiling surfaces this however is an important property. Firstly, a significant fact is that higher contact angles do not always correlate with smaller sliding angles [76], meaning that the term hydrophobicity has been used in cases where perhaps the ‘true’ repellency of water has not been present. Secondly, it has been reported that if the surface really repels the droplet on it the contact angle hysteresis (θ_A-θ_R) is small and the drop moves spontaneously or easily on horizontal or near-horizontal surfaces [77]. Our results in Papers IV and V are in agreement with the aforementioned.

The first statement is observed with e.g. PTFE and also with DLC-PTFE-h coatings. These materials have high contact angles and they are said to be hydrophobic, but their sliding angles are far from low and water droplets stick on them. The second statement is in

agreement with the results of Paper V (see V, Table 1): in DLC-PDMS-h coatings high contact angles and extremely low sliding angles (and small contact angle hysteresis) have been measured.

An extremely low sliding angle of only 0.15°±0.03° was measured with the 20 µl distilled water droplet on the surface of DLC-PDMS-h coating. A sliding angle of only 0.15° is exceptional, for instance in [78] Miwa et al. reported a sliding angle of ~1° for a 7 mg water droplet on a surface made out of a boehmite (AlOOH) ethanol mixture coated with a thin layer of hydrophobic fluroalkysilane. They also state that it is the lowest sliding angle value ever reported for solid surface. The gravitational force moving the 7 mg droplet is twice the force affecting to the 20 µl droplet. The roughness of the boehmite coatings was 59 nm and the film surface had a needle-like structure of sharp islands which is thought to lead to very low sliding angle, as the droplet sliding down the surface hardly touches the surface but moves on an air cushion. The RMS roughnesses of the DLC-p-h coatings are typically 20-30 nm and no needle-like structure exists. The ultrahydrophobic surfaces with contact angles much higher than 120° and even with low sliding angles are gained with extreme surface topography, whose failure points are their ageing and decay under demanding conditions. This is not the case with the novel DLC-polymer-hybrid coatings.

4 CONCLUSIONS

High-quality and ultra-thick diamond-like carbon coatings can save money and human lives e.g. as a protective coating on artificial hip joints. The novel hybrid coatings are promising materials of the future. Their possible applications are tied with various places where they could be used for preventing surfaces from getting dirty: e.g. kitchens, food industry’s apparatus and hospitals. Hybrid coatings are being tested in several applications: in different molds enhancing the properties of the final product and extending the life time of the mold, in different biomedical devices and tools and even as a biomaterial in places where the adhesion of bacteria or unwanted cells have to be avoided.

Large amount of experimental work has been done in order to understand and optimize the deposition process of diamond-like carbon (DLC) with the filtered pulsed arc discharge (FPAD) method. Ultra-thick (up to 200 μm), high-quality (amount of sp^3 diamond bonds >80%) DLC coatings with superior adhesion and can be deposited with the FPAD method. A modification of the FPAD deposition system has led to the development of a totally new group of materials, namely DLC-polymer-hybrid coatings. The novel coatings can be made water and oil repellent with suitable polymers, such as the polydimethylsiloxane (PDMS). DLC-PDMS-h coatings that are hard and hydrophobic have been successfully prepared. These coatings have low sliding angles for water and oil, furthermore, they cannot be marked with common marker pens and oil drops slide down their surface leaving no trace on them.

NOMENCLATURE

DLC	Diamond-like carbon, a general term for carbon material with some sp^3 diamond bonds.
ta-C	Tetrahedral amorphous carbon, a term used to describe carbon material with significant amount (>80%) of sp^3 diamond bonds ('tetrahedrally bonded') and amorphous structure (having no long range order).
AD	Amorphous diamond, a term used to describe amorphous carbon material with properties similar to diamond.
Amorphous	No long range order, without any real or apparent crystallity.
DLC-p-h	Diamond-like carbon - polymer -hybrid, a novel coating developed at the Helsinki University Diamond Group, a coating with polymer and carbon with diamond bonds.
PDMS	Polydimethylsiloxane, polymer best known from silicone rubbers, chemical formula $[(CH_3)_2\text{-Si-O}]_n$.
PTFE	Polytetrafluoroethylene, polymer best known by the trade name teflon®, chemical formula $[CF_2]_n$.
DLC-PDMS-h	Diamond-like carbon - polydimethylsiloxane -hybrid, a coating with polydimethylsiloxane and carbon with diamond bonds.
DLC-PTFE-h	Diamond-like carbon - polytetrafluoroethylene -hybrid, a coating with polytetrafluoroethylene (teflon®) and carbon with diamond bonds.
FPAD method	Filtered pulsed arc discharge method, the deposition method developed at the Helsinki University Diamond Group.
PVD	Physical vapor deposition, methods in which the film deposition occurs via physical processes through the gas phase.
CVD	Chemical vapor deposition, methods in which the film deposition occurs via chemical processes through the gas phase.
PIXE	Proton induced X-ray emission, materials analysis technique, where proton beam targeted to the sample under examination excites the sample atoms so that they will emit characteristic X-rays and by detecting and identifying these, the elemental analysis can be conducted.

XPS	X-ray photoelectron spectroscopy, materials analysis technique, where X-rays targeted to the sample under examination cause emission of electrons. Measuring the energies of the electrons the elemental analysis and identification of chemical bonds can be done (the binding energies of the electrons depend not only on the element they are associated with but also on the chemical environment of the element).
EELS	Electron energy loss spectroscopy, materials analysis technique, where electron beam passing through the sample (thickness 10-20 nm) loses its energy in collision processes. The energy loss depends on the atoms in the sample and their chemical environment.
TOF	Time-of-flight, energy measurement method in which the time-of-flight between certain points of known distance is measured.
CCD	Charge-coupled device, a semiconductor device that is used as an optical sensor, stores charge and transfers it sequentially to an amplifier and detector.
AISI 316L	Stainless steel alloy, contains iron and 18% chromium, 10% nickel and 3% molybdenum.
EMP	Electromagnetic pulse, high-intensity, short-duration burst of electromagnetic energy.
Plasma	Fourth form of matter, gas-like collection of charged particles.

ACKNOWLEDGEMENTS

I wish to thank the former and current heads of Accelerator Laboratory, Doc. Eero Rauhala and Prof. Jyrki Räisänen for placing the facilities of the laboratory at my disposal. I also thank the head of the Department of Physical Sciences, Prof. Juhani Keinonen for the opportunity to conduct research at the department.

I wish to express my sincere gratitude to my supervisor Prof. Asko Anttila for his expert guidance and enthusiasm for experimental research work. I would also like to thank my colleagues at the Accelerator Laboratory and outside world and especially Diamond Group for providing valuable discussions and entertaining events.

Warm thanks to my family and friends and especially to Kari for supporting me and for building our house.

Financial support from the National Graduate School of Materials Physics, Magnus Ehrnrooth, the Väisälä and Olga Leikola Foundations as well as the University of Helsinki Chancellor's travel fund is gratefully acknowledged.

Helsinki, March 2004
Mirjami Kiuru

REFERENCES

1. S. Aisenberg and R. Chabot, *Ion beam deposition of thin films of diamondlike carbon*, J. Appl. Phys. **42**, 2953 (1971).

2. J. Robertson, *Requirements of ultrathin carbon coatings for magnetic storage technology*, Tribology Intern. **36**, 405 (2003).

3. A. Ferrari, *Diamond-like carbon for magnetic storage disks*, Surf. Coat. Technol. **180-181**, 190 (2004).

4. M. Chhowalla, *Thick, well-adherent, highly stressed tetrahedral amorphous carbon*, Diamond Relat. Mater. **10**, 1011 (2001).

5. V-M. Tiainen, *Protection of industrial sensors with ta-C*, Vacuum **67**, 599 (2001).

6. R. Lappalainen, H. Heinonen, A. Anttila, S. Santavirta, *Some relevant issues related to the use of amorphous diamond coatings for medical applications*, Diamond Relat. Mater. **7**, 482 (1998).

7. A. Anttila, R. Lappalainen, H. Heinonen, S. Santavirta, Y. T. Konttinen, *Superiority of diamondlike carbon coatings on articulating surfaces of artificial hip joint*, New Diam. Front. C. Tech. **9**, 283 (1999).

8. V-M. Tiainen, *Amorphous carbon as a bio-mechanical coating – mechanical properties and biological applications*, Diamond Relat. Mater. **10**, 153 (2001).

9. R. Lappalainen, M. Selenius, A. Anttila, Y. T. Konttinen, S. Santavirta, *Reduction of wear in total hip replacement prostheses by amorphous diamond coatings*, J. Biomed. Mater. Res. Part B: Appl. Biomater. **66**B, 410 (2003).

10. A. Grill, *Diamond-like carbon coatings as biocompatible materials - an overview*, Diamond Relat. Mater. **12**, 166 (2003).

11. R. Hauert, *A review of modified DLC coatings for biological applications*, Diamond Relat. Mater. **12**, 583 (2003).

12. J. Robertson, *Diamond-like amorphous carbon*, Mat. Sci. Eng. R. **37**, 129 (2002).

13. J.E. Field, The Properties of Diamond (Academic Press, London, 1979) p.641-653.

14. P.J. Fallon, V.S. Veerasamy, C.A. Davis, J. Robertson, G.A.J. Amaratunga, W.I. Milne, J. Koskinen, *Properties of filtered-ion-beam-deposited diamondlike carbon as a function of ion energy*, Phys Rev. B **48**, 4877 (1993).

15. T.A. Friedmann, J.P. Sullivan, J.A. Knapp, D.R. Tallant, D.M. Follstaedt, D.L. Medlin, P.B. Mirkamiri, *Thick stress-free amorphous tetrahedral carbon films with hardness near that of diamond*, Appl. Phys. Lett. **71**, 3820 (1997).

16. D. R. McKenzie, *Tetrahedral bonding in amorphous carbon*, Rep. Prog. Phys. **59**, 1611 (1996).

17. Y. Lifshitz, *Diamond-like carbon - present status*, Diamond Relat. Mater. **8**, 1659 (1999).

18. A. Anttila: in 'Structure-Property Relationships in Surface-Modified Ceramics, NATO ASI Series', ed. C. J. McHargue *et al.*, p.455-475 (Kluwer, The Netherlands 1989) p.455-475.

19. J.-P. Hirvonen, J. Koskinen, R. Lappalainen, A. Anttila, *Preparation and properties of high density hydrogen free hard carbon films with direct ion beam or arc discharge deposition*, Materials Science Forum **52-53**, 197 (1989).

20. A. Anttila, J.-P. Hirvonen, J. Koskinen, *Procedure and apparatus for the coating of materials by means of a pulsating plasma beam*, US Patent 5078848 (1992).

21. M. Hakovirta, J. Salo, A. Anttila, R. Lappalainen, *Graphite particles in the diamond-like a-C films prepared with the filtered pulsed arc-discharge method*, Diamond Relat. Mater. **4**, 1335 (1995).

22. M. Hakovirta, I. Koponen, R. Lappalainen, A. Anttila, *Protrusions on the surface of of graphite cathode used in the tetrahedral amorphous carbon film deposition*, Diamond Relat. Mater. **7**, 23 (1998).

23. A. Anttila, R. Lappalainen, V-M. Tiainen, M. Hakovirta, *Superior attachment of high-quality hydrogen-free amorphous diamond films to solid materials*, Adv. Mater. **9**, 1161 (1997).

24. A. Anttila, J. Salo, R. Lappalainen, *High adhesion of diamond-like films achieved by the pulsed arc-discharge method*, Mater. Lett. **24**, 153 (1995).

25. J. Salo, R. Lappalainen, A. Anttila, *Energies of carbon plasma beams in the deposition of diamond-like coatings with the pulsed-arc-discharge method*, Appl. Phys. A **61**, 353 (1995).

26. J. Salo, *An opto-electronic method for measurement of plasma beams generated by the pulsed arc-discharge method*, Nucl. Instr and Meth. B **95**, 119 (1995).

27. M. Hakovirta, J. Salo, R. Lappalainen, A. Anttila, *Correlation of carbon ion energy with sp^2/sp^3 ratio in amorphous diamond films produced with a mass-separated ion beam*, Phys. Lett. A **205**, 287 (1995).

28. M-P. Delplancke-Ogletree, O.R. monteiro, *Measurement of stresses in diamond-like carbon films*, Diamond Relat. Mater. **12**, 2119 (2003).

29. J. Robertson, *Amorphous carbon*, Adv. Phys. **35**, 317 (1986).

30. K. Nordlund, private communication.

31. D.W. Brenner, *Empirical potential for hydrocarbons for use in simulating the chemical vapor deposition of diamond films*, Phys. Rev. B **42**, 9458 (1990).

32. D.R. McKenzie, D. Muller, B.A. Pailthorpe, *Compressive-stress-induced formation of thin-film tetrahedral amorphous carbon*, Phys. Rev. Lett. **67**, 773 (1991).

33. M. Ohring, The Materials Science of Thin Films (Academic Press, Inc., San Diego, 1992) p.109-132.

34. J. Black, *Biological performance of tantalum*, Clin. Mater. **16**, 167 (1994).

35. S.L. Lee, M. Cipollo, D. Windover, C. Rickard, *Analysis of magnetron-sputtered tantalum coatings versus electrochemically deposited tantalum from molten salt*, Surf. Coat. Technol. **120-121**, 44 (1999).

36. D.W. Matson, E.D. McClanahan, S.L. Lee, D. Windover, *Properties of thick sputtered Ta used for protective gun tube coatings*, Surf. Coat. Technol. **146-147**, 344 (2001).

37. E. Alakoski, M. Kiuru, A. Soininen, V-M. Tiainen, A. Anttila, R. Lappalainen, *Tantaalin käyttö suojaavana välikerroksena PVD-timanttipinnoitteiden alla*, FI-patent application 12.3.2002, application number 20020463.

38. A. Anttila, J. Räisänen, R. Lappalainen, *On the optimization of external PIXE arrangement*, Nucl. Instrum. Meth. B **12**, 245 (1985).

39. R. Lappalainen, L. Kaartinen, K. Veijalainen, P.L. Kuosa, S. Sankari, S. Pyörälä, M. Sandholm, S*equential changes of mineral and trace elements in milk during the course of endotoxin-induced mastitis as analyzed by particle induced -X-ray (PIXE), -gamma-ray emission (PIGE) and ion selective electrodes*, J Vet. Med. B **35**, 664 (1988).

40. S.A.E. Johansson, J.L. Campbell, Pixe, A Novel Technique for Elemental Analysis (John Wiley & Sons Inc., New York, 1988) p.1-341.

41. H. Matsuno, A. Yokoyama, F. Watari, M. Uo, T. Kawasaki, *Biocompatibility and osteogenesis of refractory metal implants, titanium, hafnium, niobium, tantalum and rhenium*, Biomaterials **22**, 1253 (2001).

42. S. Xu, D. Flynn, B.K. Tay, S. Prawer, K.W. Nugent, S.R.P. Silva, Y. Lifshits, W.I. Milne, *Mechanical properties and raman spectra of tetrahedral amorphous carbon films with high sp3 fraction deposited using a filtered cathodic arc*, Phil. Mag. B **76**, 351 (1997).

43. M. Chhowalla, J. Robertson, C.W. Chen, S.R.P. Silva, C.A. Davis, G.A.J. Amaratunga, W.I. Milne, *Influence of ion energy and substrate temperature on the optical and electronic properties of tetrahedral amorphous carbon (ta-C) films*, J. Appl. Phys. **81**, 139 (1997).

44. G. Fiksel, D.J. Den Hartog, P.W. Fontana, *An optical probe for local measurements of fast plasma ion dynamics*, Rev. Sci. Instrum. **69**, 2024 (1989).

45. W.D. Davis, H.C. Miller, *Analysis of the electrode products emitted by dc arcs in a vacuum ambient*, J. Appl. Phys. **40**, 2212 (1969).

46. I.I. Aksenov, S.I. Vakula, V.G. Padalka, V.E. Strel´nitskii, V.M. Khoroshikh, *High-efficiency source of pure carbon plasma*, Sov. Phys.-Tech. Phys. **25**, 1164 (1980).

47. I.G. Brown, B. Feinberg, J. E. Galvin, *Multibly stripped ion generation in the metal vapor vacuum arc*, J. Appl. Phys. **63**, 4889 (1988).

48. I.G. Brown, X. Godechot, *Vacuum arc ion charge-state distributions*, IEEE Trans. Plasma Sci. **19**, 713 (1991).

49. Anders, *A periodic table of ion charge-state distributions observed in the transition region between vacuum sparks and vacuum arcs*, IEEE Trans. Plasma Sci. **29**, 393 (2001).

50. CRC Handbook of Chemistry and Physics, 82nd edn., ed. D.R. Lide, (CRC Press, New York, 2001) Section 10, p.1-87 and p.175.

51. A.R. Striganov, N.S. Sventitskii, Tables of Spectral Lines of Neutral and Ionised Atoms, (Plenum, New York, 1968) p.92-110.

52. E. Alakoski, M. Kiuru, A. Soininen, V-M. Tiainen, A. Anttila, R. Lappalainen, *Timanttisidoksiset hiili-polymeerimateriaalit*, FI-patent application 12.3.2002, application number 20020462.

53. R. Blossey, *Self-cleaning surfaces – virtual realities*, Nature Mater. **2**, 301 (2003).

54. A. Nakajima, K. Hashimoto, T. Watanabe, *Recent studies on hydrophobic films*, Monatsh. Chem. **132**, 31 (2001).

55. A. Nakajima, A. Fujishima, K. Hashimoto, T. Watanabe, *Preparation of transparent superhydrophobic boehmite and silica films by sublimation of aluminium acetylacetonate*, Adv. Mater. **11**, 1365 (1999).

56. Y. Taga, *Recent progress in coating technology for surface modification of automotive glass*, J. Non-Cryst. Solids **218**, 335 (1997).

57. J. Tsibouklis, M. Stone, A. A. Thorpe, P. Graham, T.G. Nevell, R. J. Ewen, *Inhibiting bacterial adhesion onto surfaces: the non-stick coating approach*, Int. J. Adhesion Adhesives **20**, 91 (2000).

58. J. H. Clint, A. C. Wicks, *Adhesion under water: surface energy considerations*, Int. J. Adhesion Adhesives **21**, 267 (2001).

59. B. Janocha, D. Hegemann, C. Oehr, H. Brunner, F. Rupp, J. Geis-Gerstorfer, *Adsorption of protein on plasma-polysiloxane layers of different surface energies*, Surf. Coat. Tech. **142-144**, 1051 (2001).

60. J.-D. Kim, K.-H. Lee, K.-Y. Kim, H. Sugimura, O. Takai, Y. Wu, Y. Inoue, *Characteristics and high water-repellency of a-C:H films deposited by r.f. PECVD*, Surf. Coat. Tech. **162**, 135 (2003).

61. H. Ji, A. Côté, D. Koshel, B. Terreault, G. Abel, P. Ducharme, G. Ross, S. Savoie, *Hydrophobic fluorinated carbon coatings on silicate glaze and aluminum*, Thin Solid Films **405**, 104 (2002).

62. K. Huikko, P. Östman, K. Grigoras, S. Tuomikoski, V-M. Tiainen, A. Soininen, K. Puolanne, A. Manz, S. Franssila, R. Kostiainen, T. Kotiaho, *Poly(dimethylsiloxane) electrospray devices fabricated with diamond-like carbon – poly(dimethylsiloxane) coated SU-8 masters*, Lab Chip **3**, 67 (2003).

63. T. Young, *An Essay on the Cohesion of Fluids*, Philos. Trans. R. Soc. London **95**, 65 (1805).

64. D.Y. Kwok, A.W. Neumann, *Contact angle measurement and contact angle interpretation*, Adv. Colloid Interface Sci. **81**, 167 (1999).

65. R.N. Wenzel, *Resistance of solid surfaces to wetting by water*, Ind. Eng. Chem. **28**, 988 (1936).

66. A.B.D. Cassie, S. Baxter, *Wettability of porous surface*, Trans. Faraday Soc. **40**, 546 (1944).

67. R.E. Johnson, R.H. Dettre, *Contact angle, wettability and adhesion*, Adv. Chem. Ser. **43**, 112 (1964).

68. P.S. Swain, R. Lipowski, *Contact angles on heterogenous surfaces: a new look at Cassie's and Wenzel's laws*, Langmuir **14**, 6772 (1998).

69. D. Öner, T.J. McCarthy, *Ultrahydrophobic surfaces. Effects of topography length scales on wettability*, Langmuir **16**, 7777 (2000).

70. S. Brandon, N. Haimovich, E. Yeger, A. Marmur, *Partial wetting of chemically patterned surfaces: the effect of drop size*, J. Colloid Interface Sci. **263**, 237 (2003).

71. J.P. Youngblood, T.J. McCarthy, *Ultrahydrophobic Polymer Surfaces Prepared by Simultaneous Ablation of Polypropylene and Sputtering of Poly(tetrafluoroethylene) Using Radio Frequency Plasma*, Macromolecules **32**, 6800 (1999).

72. Z. Yoshimitsu, A. Nakajima, T. Watanabe, K. Hashimoto, *Effects of Surface Structure on the Hydrophobicity and Sliding Behavior of Water Droplets*, Langmuir **18**, 5818 (2002).

73. T. Nishino, M. Meguro, K. Nakamae, M. Matsushita, Y. Ueda, *The Lowest Surface Free Energy Based on -CF_3 Alignment*, Langmuir **15**, 4321 (1999).

74. W. Barthlott, C. Neinhuis, *Purity of sacred lotus, or escape from contamination in biological surfaces*, Planta **202**, 1 (1997).

75. A. Lafuma, D. Quéré, *Superhydrophobic states*, Nature Mater. **2** 457 (2003).

76. H. Murase, T. Fujibayashi, *Characterization of molecular interfaces in hydrophobic systems*, Prog. Org. Coat. **31**, 97 (1997).

77. W. Chen, A.Y. Fadeev, M.C. Hsih, D. Öner, J. Youngblood, T.J. McCarthy, *Ultrahydrophobic and Ultralyophobic Surfaces: Some Comments and Examples*, Langmuir **15**, 3395 (1999).

78. M. Miwa, A. Nakajima, A. Fujishima, K. Hashimoto, T. Watanabe, *Effects of the Surface Roughness on Sliding Angles of Water Droplets on Superhydrophobic Surfaces*, Langmuir **16**, 5754 (2000).